Energy-dependent separable potentials*

D. J. Ernst
Department of Physics, Case Western Reserve University, Cleveland, Ohio 44106

J. T. Londergan
Department of Physics, Indiana University, Bloomington, Indiana 47401

E. J. Moniz
Laboratory for Nuclear Science and Department of Physics, Massachusetts Institute of Technology, Cambridge, Massachusetts 02139

R. M. Thaler
Department of Physics, Case Western Reserve University, Cleveland, Ohio 44106
(Received 13 June 1974)

A method for constructing energy-dependent separable potentials of the form $V = \lambda(E)|v\rangle\langle v|$ from (complex) elastic scattering phase shifts is presented. The energy-dependent coupling constant $\lambda(E)$ is shown to satisfy a dispersion relation as a consequence of the requirement of multichannel unitarity. It is this knowledge of the analytic properties of $\lambda(E)$ which makes it possible to solve the inverse problem. It is further demonstrated that in some cases the inverse problem can still be solved analytically even when the phase shift changes sign below the inelastic threshold.

I. INTRODUCTION

Separable potentials have been widely used to represent basic interactions,[1-6] in part because their use generally provides great simplification in calculation and in part because separable potentials permit simple analytic solutions of the inverse-scattering problem.[7-9]

A rank-one separable potential leads to an off-shell transition matrix which is just a function of the on-shell T matrix and the separable form factor. In the momentum representation the fully off-shell T matrix for a separable potential, $T(p,q;E(k))$, is given by

$$T(p,q;E(k))=\left[\frac{v(p)}{v(k)}\right]T(k,k;E(k))\left[\frac{v(q)}{v(k)}\right], \quad (1.1)$$

where p and q are the off-shell momenta and k the momentum corresponding to the parametric energy E, $v(p)$ is the separable potential form factor in momentum space, and $T(k,k;E(k))$ is the on-shell elastic scattering transition matrix. In this paper, we suppress the spin and isospin indices, so that Eq. (1.1) actually represents a separate equation for each angular momentum and isospin state.

Separable form factors $v(p)$ can be readily constructed from the elastic phase shifts as solutions of the standard inverse problem.[7,8] However, when inelastic channels are open, the elastic phase shift becomes complex and the separable form factors $v(p)$ become complex, even below the threshold for inelastic scattering. Although the form factors still reproduce the on-shell scattering amplitude, they can lead to an unphysical off-shell T matrix. Calculations of pion-nucleon separable potentials[5,6] have sometimes produced off-shell T matrices which showed unphysically rapid off-shell variation, and it has been shown[9,10] that such behavior is correlated with strong absorption from the elastic channel.

As is well known,[11] the presence of inelastic channels requires an explicitly *energy-dependent* effective one-channel potential. In order to take into account the energy dependence resulting from the coupling to inelastic channels while still retaining the simplicity of a rank-one separable form factor, Londergan and Moniz[9] used an effective one-channel potential of the form

$$V_{\rm eff}(E)=\lambda_{11}\gamma(E)\,|v\rangle\langle v|=\lambda(E)\,|v\rangle\langle v|\,, \quad (1.2)$$

where $\lambda(E)\equiv\lambda_{11}\gamma(E)$ was taken to be an energy-dependent coupling constant obtained by formal elimination of the coupled inelastic channels and λ_{11} denoted the sign of the interaction, i.e., $\lambda_{11}=\pm 1$. It is the purpose of this paper to show that an energy-dependent rank-one separable potential of the form of Eq. (1.2) can be constructed under much more general circumstances than were assumed in Ref. 9.

In this section, we briefly outline our results for the inverse-scattering problem. The validity of the assumptions, and the physical conditions under which this solution can be applied, are discussed in detail in the body of the paper. If the effective one-channel potential is of the form given by Eq. (1.2), the elastic scattering matrix can then be written as

$$T(p,q;E)=\frac{\lambda_{11}v(p)v(q)}{\mathfrak{D}(E^+)}\,, \tag{1.3}$$

where

$$\mathfrak{D}(E)=[\gamma(E)]^{-1}-\lambda_{11}\int\frac{d\vec{t}}{(2\pi)^3}\,\frac{v^2(t)}{E-E(t)}\,. \tag{1.4}$$

The second term of Eq. (1.4) is analytic on the first sheet of the E plane cut above the elastic threshold energy E_0. If $[\gamma(E)]^{-1}$ is also analytic in the cut E plane, then we can write a dispersion relation for $\ln\mathfrak{D}(E^+)$, viz.

$$\ln[\mathfrak{D}(E^+)]=\frac{1}{\pi}\int_{E_0}^{\infty}\frac{dE'\,\mathrm{Im}[\ln\mathfrak{D}(E')]}{E'-E^+}\,. \tag{1.5}$$

Since $v(k)$ is a real form factor, Eq. (1.3) gives the relation

$$\mathrm{Im}[\ln\mathfrak{D}(E^+)]=-\hat{\delta}(E)\,, \tag{1.6}$$

where $\hat{\delta}(E)$ is the (real) phase of the on-shell elastic scattering amplitude, defined through

$$T(k,k;E(k))\equiv\pm\,|T(E)|\,e^{i\hat{\delta}(E)}\,, \tag{1.7}$$

with the sign in Eq. (1.7) chosen such that $\hat{\delta}(E)=\delta(E)$ below inelastic threshold. These considerations lead to the result

$$\lambda_{11}v^2(k)=\pm|T(E)|\exp\left[\frac{\mathcal{P}}{\pi}\int_{E_0}^{\infty}\frac{\hat{\delta}(x)dx}{E-x}\right]. \tag{1.8}$$

In order to use the inversion procedure described above, the phase $\hat{\delta}(E)$ must satisfy certain conditions which are listed in Eq. (2.28). If $\hat{\delta}(E)$ satisfies these conditions, then the inversion procedure of Eq. (1.8) will produce a unique rank-one separable form factor $v(k)$, which will exactly reproduce the elastic phase shift at all energies and which is consistent with the requirements of off-shell unitarity. From the prescription given above, we can also construct the energy-dependent coupling constant $\gamma(E)$. We observe that the coupling constant $\gamma(E)$ can exhibit structure even when the absorption from the elastic channel is relatively weak. For example, in Fig. 1 we plot $\gamma(E)$ for the $P_{33}\pi N$ partial wave. The phase shifts used were those which were used in Ref. 10.

In Sec. II of this paper we review in detail the assumptions and conditions which lead to the solution of the inverse problem for separable potentials. In Sec. III we present some illustrative examples to show the wide range of coupled-channel problems for which this method is applicable. In Sec. IV we show how the solution presented can be generalized by removing some of the restrictions on the phase shifts $\hat{\delta}(E)$; the technical details of this extension are further described in an Appendix.

II. INVERSE SCATTERING PROBLEM

We begin by assuming the existence of an underlying Hermitian Hamiltonian H and a corresponding

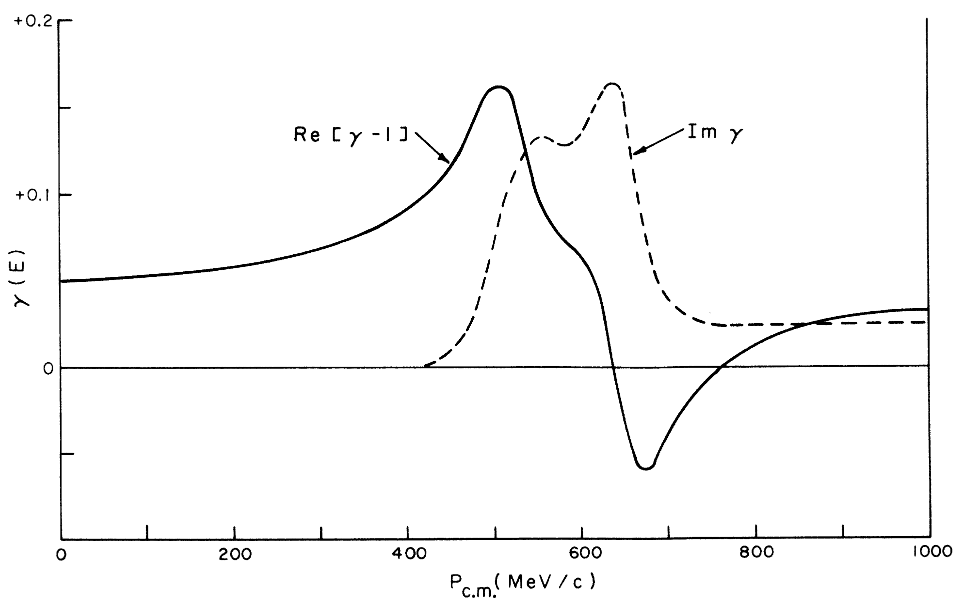

FIG. 1. The energy-dependent coupling parameter $\gamma(E)$ for the effective potential which produces the experimental phase shifts for elastic pion-nucleon scattering in the P_{33} channel. The phase shifts used in the inverse problem and the resulting $v(k)$ are given in Ref. 10.

Hermitian potential V. This Hamiltonian is assumed to be capable of describing the interaction in all channels of the system under discussion. We further assume that the motion of the system is completely described by a Lippmann-Schwinger operator equation of the form

$$T = V + VG^{(+)}T \,, \tag{2.1}$$

in which T is the transition operator, V is the interaction potential operator, and $G^{(+)}$ is the many-body propagator corresponding to outgoing flux in each open channel.

We now define both a projection operator P, with the property that P projects onto the elastic channel only, and the conjugate projection operator[11] $Q = 1 - P$. Then, we may easily obtain from Eq. (2.1) a Lippmann-Schwinger equation for the elastic channel alone, viz.

$$PTP = P\mathcal{V}_{\text{eff}}P + P\mathcal{V}_{\text{eff}}PG^{(+)}PTP \,, \tag{2.2}$$

where

$$\mathcal{V}_{\text{eff}}(E) = V + VQ\mathcal{G}^{(+)}QV \tag{2.3}$$

and

$$\begin{aligned}\mathcal{G}^{(+)}(E) &= QG^{(+)}Q[1 - QVQG^{(+)}Q]^{-1_Q} \\ &= Q[E - QHQ]^{-1_Q}Q \,. \end{aligned} \tag{2.4}$$

The superscript -1_Q in Eq. (2.4) refers to an inverse in the Q space. In Eq. (2.4) the Green's function $\mathcal{G}^{(+)}$ is specified for outgoing-wave boundary conditions in all open channels.

It is clear from Eqs. (2.3)–(2.4) that $\mathcal{V}_{\text{eff}}$ will have an explicit energy dependence resulting from formal elimination of the coupled channels. In order to retain the separability of the effective interaction, we insist that

$$\mathcal{V}_{\text{eff}}(E) = \lambda_{11}\gamma(E)\,|v\rangle\langle v| \,, \tag{2.5}$$

that is, we completely absorb the energy dependence of $\mathcal{V}_{\text{eff}}$ into the coupling constant $\gamma(E)$. If we like, we can simply take as an ansatz that the effective one-channel potential has the form of Eq. (2.5), with no reference to the explicit form of the many-channel interaction which led to that equation. However, it is clear that Eq. (2.5) will follow from any many-channel potential of the form

$$\begin{aligned} PVQ &= P\,|v\rangle\langle w|\,Q \,, \\ QVP &= Q\,|w\rangle\langle v|\,P \,, \end{aligned} \tag{2.6}$$

where $|w\rangle$ is a vector in the space defined by Q. In the usual channel notation, this implies a Hermitian potential of the form

$$V = \begin{bmatrix} \lambda_{11}|v_1\rangle\langle v_1| & \lambda_{12}|v_1\rangle\langle v_2| & \lambda_{13}|v_1\rangle\langle v_3| & \cdots \\ \lambda_{12}^*|v_2\rangle\langle v_1| & V_{22} & V_{23} & \cdots \\ \lambda_{12}^*|v_3\rangle\langle v_1| & V_{32} & V_{33} & \cdots \\ \vdots & \vdots & \vdots & \end{bmatrix}, \tag{2.7}$$

where V_{22}, V_{23}, etc., are completely unrestricted potentials. Under this restriction, Eq. (2.3) may be written as

$$\mathcal{V}_{\text{eff}}(E) = |v_1\rangle\langle v_1|\,[\lambda_{11} + \langle w|Q\mathcal{G}^{(+)}Q|w\rangle] \,. \tag{2.8}$$

Comparison of Eq. (2.8) with Eq. (2.5) leads to the identifications

$$|v_1\rangle\langle v_1| \equiv |v\rangle\langle v| \tag{2.9}$$

and

$$\gamma(E) = 1 + \frac{1}{\lambda_{11}}\langle w|Q\mathcal{G}^{(+)}Q|w\rangle \,. \tag{2.10}$$

The vector $|w\rangle$ is then

$$|w\rangle = \sum_{j=2}^{N} \lambda_{1j}^*\,|v_j\rangle \,, \tag{2.11}$$

and we have made no assumption about the form of the $|v_j\rangle$ which make up $|w\rangle$.

If $\langle w|Q\mathcal{G}^+(E)Q|w\rangle$ exists for all values of E, then for large $|E|$

$$\langle w|Q\mathcal{G}^{(+)}Q|w\rangle \xrightarrow[|E|\to\infty]{} 0 \tag{2.12}$$

faster than $|E|^{-1}$. This ensures that $\gamma(E) \to 1$ for

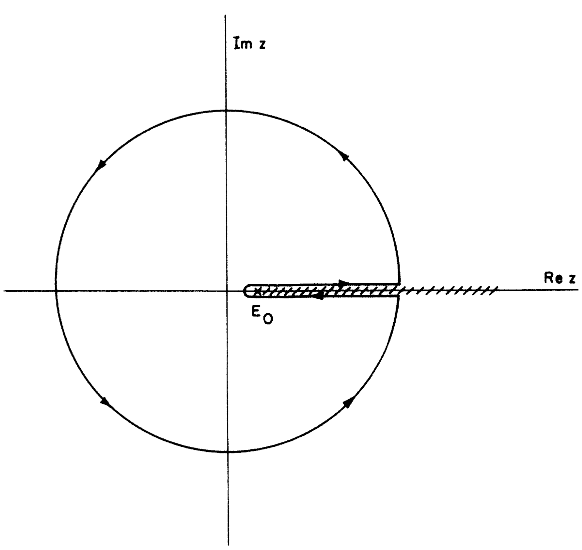

FIG. 2. The cut z plane and the contour used to derive the dispersion relation for $1/\gamma(z)$.

large values of E. From Eq. (2.4) we see that we can analytically continue $\gamma(z)$ off the real energy axis into the complex E plane. From the boundary conditions on $Q\mathcal{G}^{(+)}(E)Q$, we see that $\text{Im}\gamma(E)=0$ for real energies below the first inelastic threshold energy ϵ_i. Thus the function $\gamma(z)$ can be analytically continued into the complex E plane, cut along the real axis extending from ϵ_i to ∞. If $\gamma(z)$ can be analytically continued into the cut E plane, then so can $1/\gamma(z)$. Further, as $|z|\to\infty$, $[1/\gamma(z)]-1\to 0$ faster than $|z|^{-1}$. However, a pole of $1/\gamma(z)$ occurs wherever $\gamma(z)$ has a zero. We will return later to the question of zeroes of $\gamma(z)$, and confine ourselves to the case where $\gamma(z)$ has no zeroes in the first sheet of the z plane, cut along the real axis from inelastic threshold ϵ_i to ∞. By Cauchy's theorem, we can write

$$\frac{1}{\gamma(z)}-1=\frac{1}{2\pi i}\oint_c\frac{[1/\gamma(z')-1]dz'}{z'-z}. \qquad (2.13)$$

Choosing the path of integration to be the infinite circle with a detour about the branch cut, as shown in Fig. 2, we can neglect the contribution from the circle since $[1/\gamma(z)]-1$ vanishes at $|z|=\infty$, so that Eq. (2.13) yields the result

$$\frac{1}{\gamma(E)}=1+\frac{1}{\pi}\int_{\epsilon_i}^{\infty}\frac{\text{Im}[1/\gamma(E')]dE'}{E'-E-i\epsilon}, \qquad (2.14)$$

that is, $1/\gamma(E)$ satisfies an unsubtracted dispersion relation.

We demonstrate the implications of Eq. (2.14) for the inverse-scattering problem by examining the transition operator in the elastic channel, which takes the form

$$T=\frac{|v\rangle\langle v|}{1/\lambda(E)-\langle v|G^{(+)}(E)|v\rangle}, \qquad (2.15)$$

where $G^{(+)}$ indicates the outgoing-wave prescription for the Green's function. On the energy shell, we can solve for $1/\lambda(E)$ to obtain

$$\frac{1}{\lambda(E)}=[v(k_E)]^2\frac{1}{T(E)}+\int_{E_0}^{\infty}\frac{\mu k_{E'}[v(k_{E'})]^2dE'}{2\pi^2[E+i\epsilon-E']}. \qquad (2.16)$$

In Eq. (2.16) μ is the reduced mass[12] in the elastic channel, k_E is the momentum corresponding to energy E, $T(E)$ represents the fully on-shell T matrix $T(k_E, k_E; E)$, and E_0 denotes the elastic threshold energy. The imaginary part of Eq. (2.16) then gives

$$\text{Im}\left[\frac{1}{\lambda(E)}\right]=[v(k_E)]^2\,\text{Im}\left[\frac{1}{T(E)}\right]-\frac{\mu k_E[v(k_E)]^2}{2\pi}. \qquad (2.17)$$

Substituting this relation into Eq. (2.14), we obtain

$$\frac{1}{\gamma(E)}=1-\lambda_{11}\int_{E_0}^{\infty}\frac{[v(k_{E'})]^2\{\text{Im}[1/\pi T(E')]-\frac{1}{2}\mu k_{E'}\}dE'}{E+i\epsilon-E'}. \qquad (2.18)$$

Substitution of Eq. (2.18) into Eq. (2.15) then gives

$$T(E)=[v(k_E)]^2\Big/\left\{\lambda_{11}-\frac{1}{\pi}\int_{E_0}^{\infty}\frac{[v(k_{E'})]^2\,\text{Im}[1/T(E')]\,dE'}{E+i\epsilon-E'}\right\} \qquad (2.19)$$

for the on-shell T matrix. After multiplication of both sides of Eq. (2.19) by $\text{Im}[2\pi/\mu k_E T(E)]$ we obtain

$$\hat{T}(E)=\frac{[g(k_E)]^2}{\lambda_{11}-\langle g|G^{(+)}(E)|g\rangle}, \qquad (2.20)$$

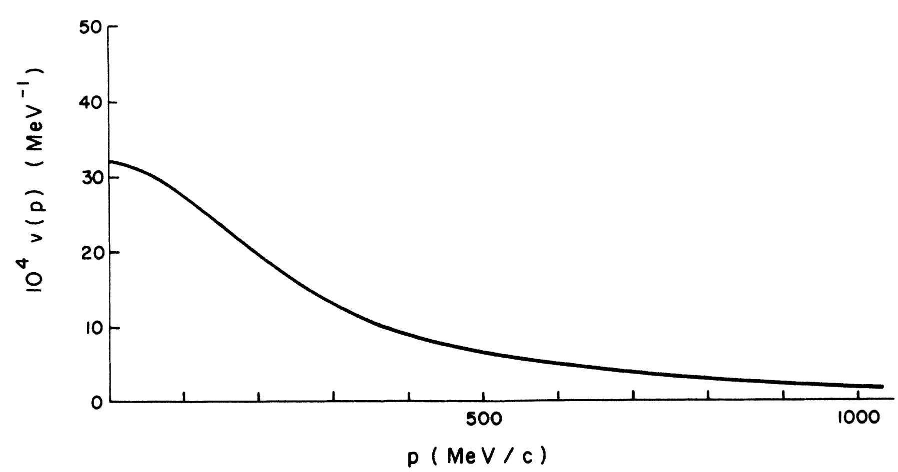

FIG. 3. The separable potential $v_1(p)$ given in Eq. (3.7). For different couplings to the inelastic channels, this potential produces phase shifts as depicted in Figs. 4–6, 13.

where in Eq. (2.20) we define

$$\hat{T}(E) \equiv T(E)\,\mathrm{Im}\left[\frac{2\pi}{\mu k_E T(E)}\right] \qquad (2.21)$$

and

$$[g(k_E)]^2 \equiv [v(k_E)]^2\,\mathrm{Im}\left[\frac{2\pi}{\mu k_E T(E)}\right]. \qquad (2.22)$$

As has been noted previously, Eq. (2.20) is a one-channel equation, since $\hat{T}(E)$ satisfies elastic unitarity, i.e., $\mathrm{Im}[1/\hat{T}(e)] = \mu k_E/2\pi$. We can then easily obtain $g(k)$ from the usual prescription[7] for solving the inverse problem for separable potentials, which is repeated here for completeness. We can write Eq. (2.20) as

$$\hat{T}(E) = \frac{\lambda_{11}[g(k_E)]^2}{D^{(+)}(E)}, \qquad (2.23)$$

where

$$D^{(+)}(E) \equiv 1 - \lambda_{11}\langle g\,|G^{(+)}(E)|g\rangle. \qquad (2.24)$$

Since $\hat{T}(E)$ satisfies elastic unitarity, we may write $\hat{T}(E)$ in terms of a real phase shift $\hat{\delta}(E)$ defined by

$$\hat{T}(E) = -\frac{2\pi}{\mu k_E}\exp[i\hat{\delta}(E)]\sin[\hat{\delta}(E)], \qquad (2.25)$$

so that, provided $\hat{\delta}(E)$ is "well-behaved," $D^{(+)}(E)$ can be constructed from the formula

$$D^{(+)}(E) = \exp\left[\frac{1}{\pi}\int_{E_0}^{\infty}\frac{\hat{\delta}(x)dx}{E+i\epsilon-x}\right]. \qquad (2.26)$$

From Eq. (2.25) and (2.26), we can calculate $g(k_E)$, and we can then solve for $v(k_E)$ from Eq. (2.22), to get

$$\lambda_{11}[v(k_E)]^2 = T(E)\exp\left[\frac{1}{\pi}\int_{E_0}^{\infty}\frac{\hat{\delta}(x)dx}{E+i\epsilon-x}\right]. \qquad (2.27)$$

The conditions, which the phase shift must satisfy in order that the inversion procedure described above apply are:

(i) $\hat{\delta}(E) \to 0$ as $E \to \infty$;

(ii) $\hat{\delta}(E_0) = 0$; (2.28)

(iii) $\sin\hat{\delta}(E)$ cannot change sign below inelastic threshold.

If $\hat{\delta}(E)$ satisfies conditions (i)–(iii), then the inversion procedure of Eq. (2.27) will produce a unique rank-one separable potential with an energy-dependent coupling constant $\gamma(E)$, defined through Eq. (2.16). Such a potential will reproduce the elastic phase shift at all energies and will be consistent with the requirements of multichannel unitarity. Further, the coupling constant $\gamma(E)$, which accompanies the separable potential $v(k)$ will have no zeroes on the first, or physical, sheet of the complex E surface and hence $1/\gamma(E)$ will satisfy the unsubtracted dispersion relation given by Eq. (2.14).

In the parametrization we have chosen, all of the information about the coupled inelastic channels goes into the coupling constant $\gamma(E)$. Changes in $\gamma(E)$ can produce dramatic changes in the elastic scattering amplitude, even when the form factor $v(p)$ remains constant. Pion-nucleon separable form factors constructed by the method described above were found[10] to be smooth functions of the

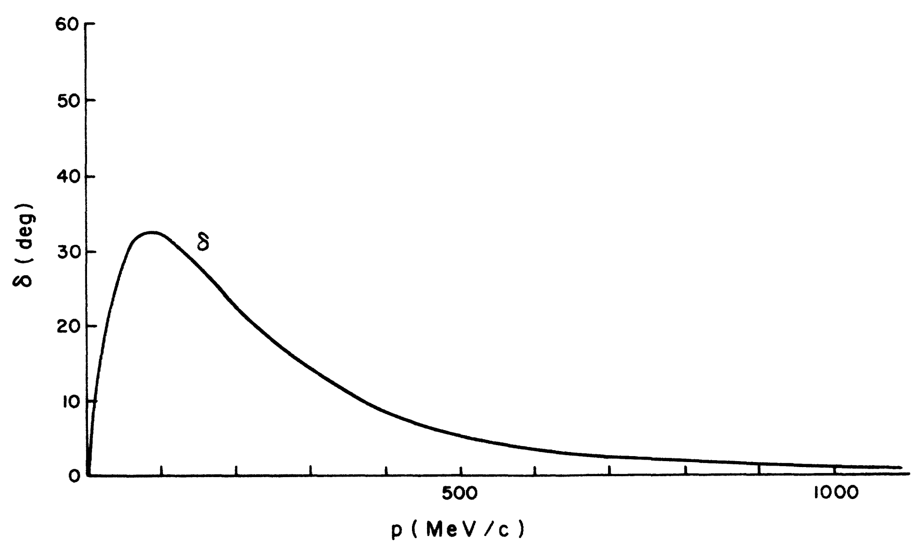

FIG. 4. The phase shift generated by the separable potential $-v_1(p)v_1(p')$ with $v_1(p)$ given by Eq. (3.7) and depicted in Fig. 3.

c.m. momentum, even when the energy dependence of the on-shell T matrix was quite pronounced.

III. SOME ILLUSTRATIVE EXAMPLES

We can illustrate the effects of changing $\gamma(E)$ by examining a two-channel model problem with separable s-wave potentials in each channel, where we keep $v_1(p)$ fixed and vary $\gamma(E)$. In the momentum representation, the potential matrix has the form

$$\langle p|V|q\rangle = \begin{bmatrix} \lambda_{11}v_1(p)v_1(q) & \lambda_{12}v_1(p)v_2(q) \\ \lambda_{12}v_2(p)v_1(q) & \lambda_{22}v_3(p)v_3(q) \end{bmatrix}. \quad (3.1)$$

Nonrelativistic kinematics was used throughout these examples, with the momentum in each channel defined through the relation

$$k_1^2 = k_2^2 + \Delta_2^2. \quad (3.2)$$

The potentials $v_i(p)$ were chosen to have Yamaguchi form factors

$$v_i(p) = \left(\frac{+\pi a_i}{\mu_1}\right)^{1/2} \frac{c_i}{p^2 + a_i^2} \quad (i = 1, 2, 3). \quad (3.3)$$

Formal elimination of the coupled channels yields an effective one-channel potential

$$\langle p|v_{11}^{\text{eff}}(E)|q\rangle = \lambda_{11}\gamma(E)v_1(p)v_1(q), \quad (3.4)$$

where

$$\gamma(E) = 1 + \frac{\lambda_{12}^2 c_2^2}{\lambda_{11}[k_2 + i\alpha_2]^2}\left\{1 - \frac{\lambda_{22}c_3^2(\alpha_2 - \alpha_3)^2}{[k_2 + i\alpha_3]^2(\alpha_2 + \alpha_3)^2}\right\} \times \left[1 - \frac{\lambda_{22}c_3^2}{(k_2 + i\alpha_3)^2}\right]^{-1}. \quad (3.5)$$

In Eq. (3.4), we define

$$\alpha_i \equiv \left(\frac{\mu_1}{\mu_2}\right)^{1/2} a_i \quad (i = 2, 3). \quad (3.6)$$

In all cases the same potential $v_1(p)$ was used, with

$$a_1 = \Delta = 250 \text{ MeV}/c$$

and

$$c_1 = 200 \text{ MeV}/c,$$

viz.

$$v_1(p) \sim \frac{200}{p^2 + (250)^2}. \quad (3.7)$$

In Fig. 3, v_1 is plotted as a function of c.m. momentum and is shown to be quite smoothly varying. In Fig. 4 is plotted the phase shift corresponding to absence of channel coupling ($\lambda_{12} = 0$), and $\lambda_{11} = 1$, which corresponds to an attractive interaction in channel 1. In Fig. 5, the parameters used are[13]

$$\lambda_{11} = \lambda_{22} = 0, \quad \lambda_{12} = 1,$$

$$c_2 = 300 \text{ MeV}/c, \quad a_2 = 400 \text{ MeV}/c.$$

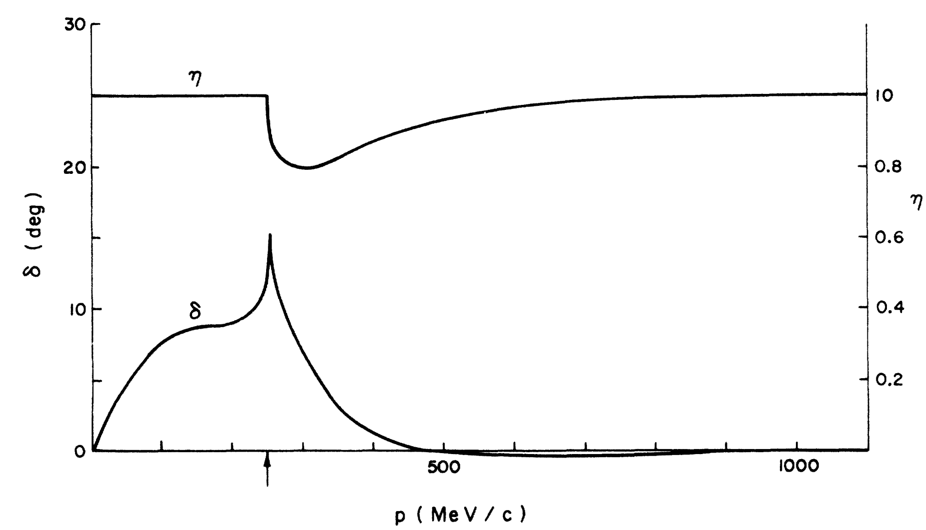

FIG. 5. The phase shift and inelasticity parameter, defined as one-half the phase and the magnitude of the S matrix, $S(k) = \eta(k)\exp[2i\delta(k)]$, for the model coupled channel problem given in Eq. (3.1). The potential $v_1(p)$ is given in Eq. (3.7) and the remaining parameters are $\lambda_{11} = \lambda_{23} = 0$, $\lambda_{12} = 1$, $c_2 = 300$ MeV/c, $\alpha_2 = 400$ MeV/c. The arrow indicates the inelastic threshold.

In Fig. 5, the direct coupling is absent in both channel 1 and 2, and only the channel coupling term remains. This term always produces an attractive effective potential in channel 1 below inelastic threshold, and produces a phase shift with a pronounced spike at the opening of the inelastic channel. In Fig. 6, the parameters are

$$\lambda_{11}=\lambda_{22}=-1, \quad \lambda_{12}=1,$$

$$c_2=150 \text{ MeV}/c, \quad \alpha_2=400 \text{ MeV}/c,$$

$$c_3=300 \text{ MeV}/c, \quad \alpha_3=250 \text{ MeV}/c,$$

These parameters correspond to a "virtual bound state" resonance; the coupling in channel 2 is strong enough to produce a bound state in channel 2, in the absence of coupling to channel 1. The channel coupling produces a sharp resonance in channel 1 below inelastic threshold. We have tested the inversion procedure numerically for the T matrices given in Figs. 3–6. *In all these cases the separable potential of Eq. (3.7), given in Fig. 3, is reproduced.*

Another application of this technique might be to nucleon-nucleon scattering. Here, the phase shifts are known accurately only up to about 350 MeV (laboratory energy); which is just below the energy at which pion production begins to become appreciable. Consequently, when the phase shift analyses are extended to higher energy, one will have to include absorptive effects in employing the additional information as a constraint of the off-shell nucleon-nucleon T matrix. We have computed the energy-dependent potential for the ${}^1D_2$ partial wave, assuming the absorption is given correctly by Amaldi's peripheral model calculation.[14] The input phase shifts are shown in Fig. 7, and the potential in Fig. 8. In order to illustrate the importance of including the absorption, we display two additional potentials (normalized to unity at 350 MeV/c). The dashed line is the potential obtained with the same phase shift δ but with the inelasticity parameter η set equal to unity at all energies, the dash-dot curve is the Tabakin potential.[15] The latter is not obtained as the solution of an inverse scattering solution but is simply an analytic form which approximately reproduces the ${}^1D_2$ phase shift below 350 MeV/c. Because of the normalization, Fig. 8 effectively represents [cf. Eq. (1.1)] the half-off-shell extrapolation of the partial wave T matrix for $k \leq 350$ MeV/c. The three extrapolations are substantially different for large off-shell momenta.

IV. GENERALIZATION OF THE INVERSE SCATTERING SOLUTION

In this section we examine the conditions on $\hat{\delta}(E)$ necessary to perform the inversion procedure.

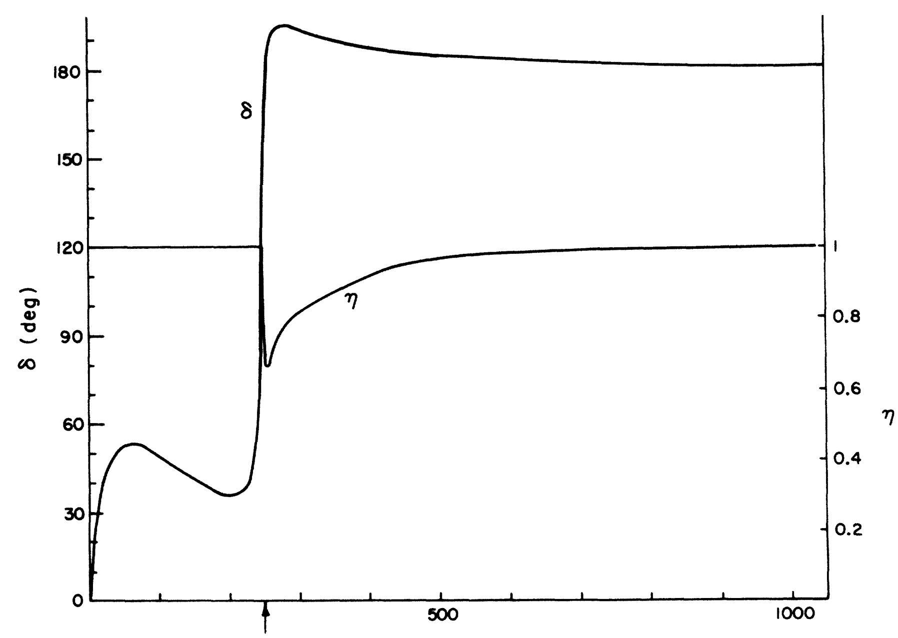

FIG. 6. The same as Fig. (5) except the parameters used are $\lambda_{11}=\lambda_{22}=-1$, $\lambda_{12}=1$, $c_2=150$ MeV/c, $\alpha_2=400$ MeV/c, $c_3=300$ MeV/c, $\alpha_3=250$ MeV/c. With these parameters the inelastic channel, if it were uncoupled to the elastic channel, would have a bound state just below the inelastic threshold. In the coupled channel problem, this produces a virtual bound state resonance just below the inelastic threshold.

We shall see that some of the restrictions given in Eq. (2.28) can be removed by an alteration of the procedure for constructing the function $D^{(+)}(E)$ [Eq. (2.26)]. The first condition is that $\hat{\delta}(E)\to 0$ as $E\to\infty$. When using experimental phase shifts, which are supplied only up to some maximum experimental energy, we can satisfy this criterion by choosing a high-energy extrapolation for the phase shift which insures $\hat{\delta}(E)\to 0$. Relaxation of the other restrictions on the phase shift requires changes in the procedure for constructing $D^{(+)}(E)$. Equation (2.26) gives the relation

$$D^{(+)}(E)=\frac{1}{\gamma(E)}-\lambda_{11}\langle v|G^{(+)}(E)|v\rangle =\exp\left[\frac{1}{\pi}\int_{E_0}^{\infty}\frac{\hat{\delta}(x)dx}{E+i\epsilon-x}\right], \tag{4.1}$$

and this relation requires that $D^{(+)}(E)$ have no zeroes and no poles on the first sheet of the cut E plane. If $\hat{\delta}(E_0)=\pi$, there is a pole of $T(E)$, and hence a zero of $D^{(\pm)}(E)$, at negative energy $E=-E_B$. A zero of the T matrix corresponds to a zero of $\gamma(E)$ [and hence a pole of $1/\gamma(E)$]. If this occurs, then $1/\gamma(E)$ will no longer satisfy an unsubtracted dispersion relation and in this case Eq. (4.1) will not obtain.

The many-channel potential given in Eq. (2.7) can lead to phase shifts in the elastic channel which are considerably more varied than would be allowed by the above conditions. We now demonstrate how the inverse problem may be solved for any set of phase shifts which could have arisen from a many-channel potential V of the form of Eq. (2.7). First, however, we must discuss the limitations on the elastic channel phase shifts implied by the existence of a many channel potential of the form of V.

The general structure of an elastic channel T matrix which arises from a potential of the form of V will be quite complicated. These complications are a result of the possible permutations of signs and the occurrence of poles and zeroes. There are, nonetheless, some general systematics in the structure of the elastic channel T matrix, which can indicate whether a given on-shell T matrix is compatible with the existence of a potential of the form of V.

We recall Eq. (2.10), which we write as

$$\lambda_{11}\gamma(E)=\lambda_{11}+\langle w|Q\mathcal{G}^{(+)}(E)Q|w\rangle . \tag{4.2}$$

If a complete set of eigenstates of QHQ is inserted into the definition of $\mathcal{G}^{(+)}(E)$, Eq. (2.4), the general form of $\lambda_{11}\gamma(E)$ is given by

$$\lambda_{11}\gamma(E)=\lambda_{11}+\sum_i\frac{|A_i|^2}{E-E_i}+\int_{\epsilon_i}^{\infty}\frac{|f(E')|^2dE'}{E-E'+i\eta}, \tag{4.3}$$

where the pole terms clearly arise from those bound states of QHQ which lie below the inelastic threshold ϵ_i. Since the inverse problem requires a dispersion relation for $1/\gamma(E)$, we must ascertain the number and the location of the zeroes of $\gamma(E)$. As a function of complex energy, $z=x+iy$,

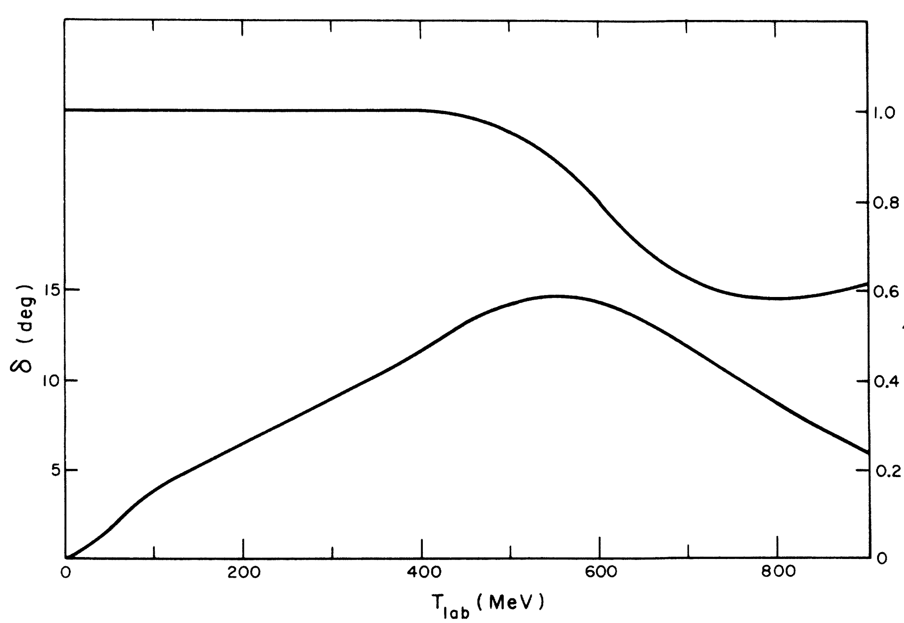

FIG. 7. The phase shift δ and the inelasticity parameter η for nucleon-nucleon scattering in the ${}^1D_2$ state. The inelasticity is calculated according to the peripheral model of Amaldi (Ref. 14).

the imaginary part of $\lambda_{11}\gamma(z)$ is given by

$$\mathrm{Im}\lambda_{11}\gamma(z) = -y\left[\sum_i \frac{|A_i|^2}{|z-E_i|^2} + \int_{\epsilon_i}^{\infty} \frac{|f(E')|^2 dE'}{|z-E'|^2}\right]. \quad (4.4)$$

Thus $\gamma(z)=0$ implies $y=\mathrm{Im}z=0$, so that all of the zeroes of $\gamma(z)$ must lie on the real axis. From Eq. (4.2), we see that $\gamma(E)$ has a negative definite imaginary part for E above inelastic threshold. Thus, all of the zeroes of $\gamma(E)$ must lie on the real axis below the inelastic threshold.[16]

At this point it is helpful to classify $\lambda_{11}\gamma(E)$ into four different classes and examine each class individually. The first is for $\lambda_{11}=+1$ (i.e., a repulsive potential in the elastic channel) and $\gamma(\epsilon_i) > 0$. The behavior of $\lambda_{11}\gamma(E)$ in this case is depicted in Fig. 9. We see that the number of zeroes of $\gamma(E)$ is exactly equal to the number of poles of $\gamma(E)$. A zero of $\gamma(E)$ implies that the energy-dependent potential $\mathcal{V}_{\mathrm{eff}}(E)$ and the elastic T matrix both pass through zero, thus the position of the zeroes of $\gamma(E)$ for energies above elastic threshold are determined by the experimental points where $\hat{\delta}(E)$ passes through $n\pi$. From Fig. 9, we see that for the case under consideration each zero of the T matrix is accompanied by a bound state pole of QHQ.

The second case we consider is again a repulsive interaction in the elastic channel ($\lambda_{11}=+1$), but with $\gamma(\epsilon_i) < 0$. The behavior of $\gamma(E)$ for this case is depicted in Fig. 10. We see that in this case the number of zeroes of $\gamma(E)$ (and of the T matrix) is one greater than the number of poles of $\gamma(E)$. In particular, we may have a zero in the T matrix without any additional singularities in $\gamma(E)$. This is possible because below threshold the integral I given by

$$I = \int_{\epsilon_i}^{\infty} \frac{|f(E')|^2 dE'}{E-E'+i\eta} \quad (4.5)$$

is always negative. Thus the effect of virtual excitations to inelastic continuum states is to produce an "attractive" effective potential below the inelastic threshold. If this "attractive" effective potential is strong enough to override the elastic channel repulsive potential, then the total potential may change from "repulsive" to "attractive" as the energy is increased.

The third case is for an attractive potential ($\lambda_{11}=-1$) in the elastic channel with $\lambda_{11}\gamma(\epsilon_i) < 0$. We have plotted $\lambda_{11}\gamma(E)$ for this case in Fig. 11. As for the first case, each zero of $\gamma(E)$ (and hence of the T matrix) is accompanied by a bound state of QHQ.

The fourth and final possibility is $\lambda_{11}=-1$ and $\lambda_{11}\gamma(\epsilon_i) > 0$. For this case, $\lambda_{11}\gamma(E)$ is depicted in Fig. 12. In this case the number of zeroes in $\gamma(E)$ is one less than the number of poles. Actual phase shifts for the case of one pole in

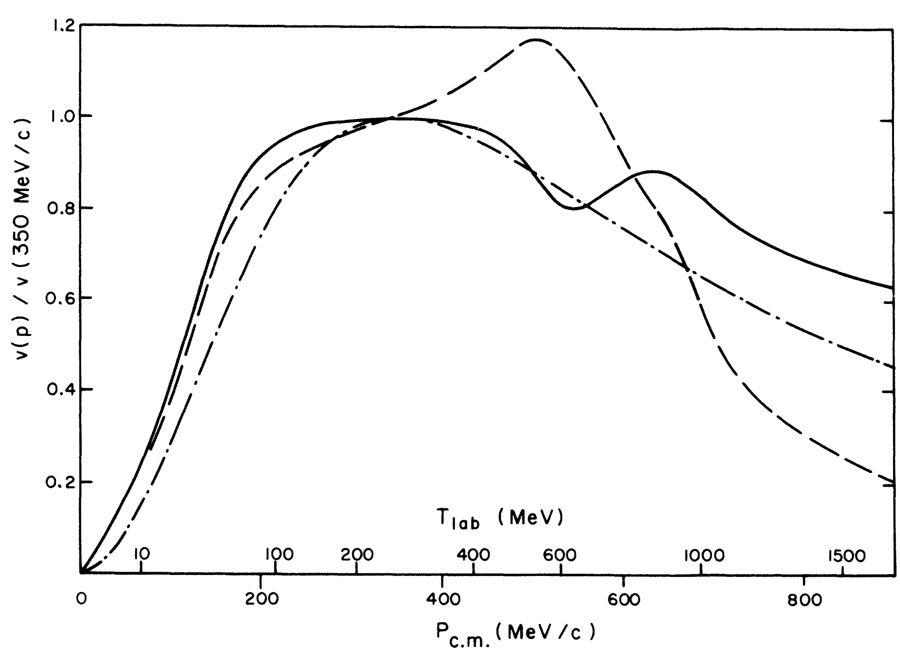

FIG. 8. The nucleon-nucleon separable potential in the $^1D_2$ state. The unbroken curve is calculated according to Eq. (2.27), while only the real phase shift δ is used to obtain the dashed curve. The dash-dot curve is the potential of Tabakin (Ref. 15).

$\gamma(E)$ and no zeroes have been given already in Fig. 5. For this case, even though $\gamma(E)$ had a pole, $1/\gamma(E)$ had no poles and the procedure for the inverse problem which we have previously outlined was applicable.

We shall now see that the construction of $v(k)$ requires the knowledge of both the poles and zeroes of $T(E)$. The zeroes of $T(E)$ are the result of $\gamma(E)$ passing through zero, the location of which we have just discussed. The structure of $T(E)$ is such that the off-shell T matrix $\langle k\,|\,T(E)\,|\,k'\rangle$ is everywhere zero if $E=\bar{E}_j$, where $\bar{E}_j$ is the location of the zero of $\gamma(E)$. The poles of $T(E)$, however, result from zeroes of the demoninator $D^{(+)}(E)$, where

$$\frac{1}{\lambda_{11}\gamma(E)}=\langle v\,|\,G^{(+)}(E)\,|\,v\rangle\,. \tag{4.6}$$

These points correspond to physical bound states of the system and are marked by $\times$ in the lower part of Figs. 9–12.

From Figs. 9–12, we have seen that the zeroes of $T(E)$ between elastic and inelastic threshold generally are associated with poles in $\gamma(E)$ due to the bound states of QHQ. The exception to this is depicted in Fig. 10 where one might have a single zero in $\gamma(E)$ [and hence $T(E)$] without a bound state of QHQ. One can further note from Figs. 9–12 that a bound state of QHQ below elastic threshold will generally lead to a zero of $D^{(+)}(E)$ [a pole of $T(E)$]. The exception to this can be seen in Fig. 10 where a bound state of QHQ [a pole in $\gamma(E)$ and a zero in $1/\gamma(E)$] is near the elastic threshold and does not result in a zero of $D^{(+)}(E)$.

The location of the zeroes of $T(E)$ below elastic threshold have no special physical significance and cannot be determined from experiment. From Figs. 9–12, one sees that one zero occurs between neighboring bound states. There may be a zero above the last bound state and below the elastic threshold as depicted in Fig. 10, or this zero may occur above the elastic threshold as depicted in Fig. 11, where its location would be observable. As the location of these zeroes in T below elastic threshold is not observable, the inverse problem loses its uniqueness in this case.[17] These required zeroes may be inserted at any location consistent with their occurrence in Figs. 9–12, but the result of the inverse problem will depend on their pre-

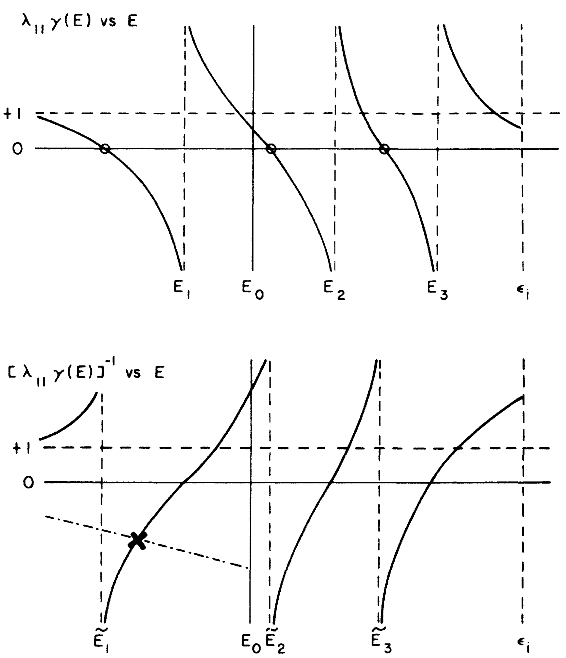

FIG. 9. In the upper graph $\lambda_{11}(E)$ is depicted for $\lambda_{11}=+1$, and for $\gamma(\epsilon_i)>0$, with ϵ_i the inelastic threshold. The case where $\gamma(E)$ has three poles at the energies E_1, E_2, and E_3 is depicted. These poles are a result of bound states of the Hamiltonian QHQ. For this case, these poles lead to zeroes of $\gamma(E)$, and hence of $T(E)$, which are marked by "O." The corresponding $[\lambda_{11}\gamma(E)]^{-1}$ is plotted in the lower graph. The dot-dash line represents $\langle v|G^{(+)}(E)|v\rangle$ for energies below elastic threshold E_0, where $\langle v|G^{(+)}(E)|v\rangle$ is real. The zero of $D^{(+)}(E)$ [a bound state pole of $T(E)$] is marked by an "×." The energies required for the inverse problem are the locations of the poles of $[\lambda_{11}\gamma(E)]^{-1}$ (here labeled $\tilde{E}_1\cdots\tilde{E}_3$ and marked by "O" in the upper graph) and the energy of the bound state (marked by "×").

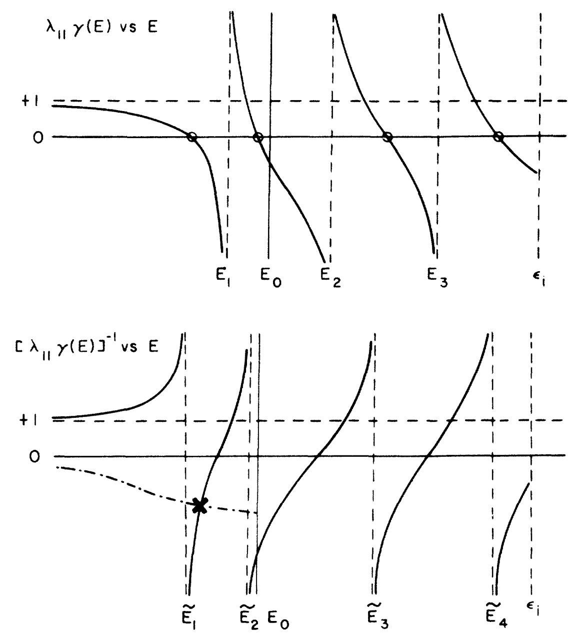

FIG. 10. The same as Fig. 9 except here the case where $\lambda_{11}=+1$ and $\gamma(\epsilon_i)<0$ is depicted. Notice that in this case the number of zeroes of $\gamma(E)$ [and $T(E)$] is one more than the number of poles of $\gamma(E)$.

cise location.

The above discussion may be seen to be consistent with Levinson's theorem. For the separable energy-dependent potential under present consideration, Levinson's theorem[18,19] is

$$\hat{\delta}(E_0) - \hat{\delta}(\infty) = (N-M)\pi\,, \qquad (4.7)$$

where N is the number of poles in the elastic channel T matrix [zeroes of $D^{(+)}(E)$] and M is the number of zeroes of the T matrix [and of $\gamma(E)$]. If the phase shifts from elastic threshold to infinity are known, the Levinson's theorem indicates the number of zeroes of $T(E)$ which occur below elastic threshold. This number must always be equal to, or one greater than or one less than, the number of bound states.

A phase shift which begins at zero, is first positive, and then changes sign and remains negative (such as the nucleon-nucleon singlet-S phase) is an example of a phase shift which is not compatible with an underlying potential of the form of Eq. (2.7). The modified Levinson's theorem of Eq. (4.7) states that for a single zero in $T(E)$ with no bound states, the phase at elastic threshold is $-\pi$. Thus one cannot have $\delta(E_0)$ start at zero, change sign, and return to zero (or $n\pi$ either) without a bound state. The addition of bound states, however, will necessarily add additional zeroes in $T(E)$ and thus even the addition of bound states cannot produce these phase shifts.

We now consider the modification of the inversion procedure which is required for the case where $D^{(+)}(E)$ has zeroes below elastic threshold,

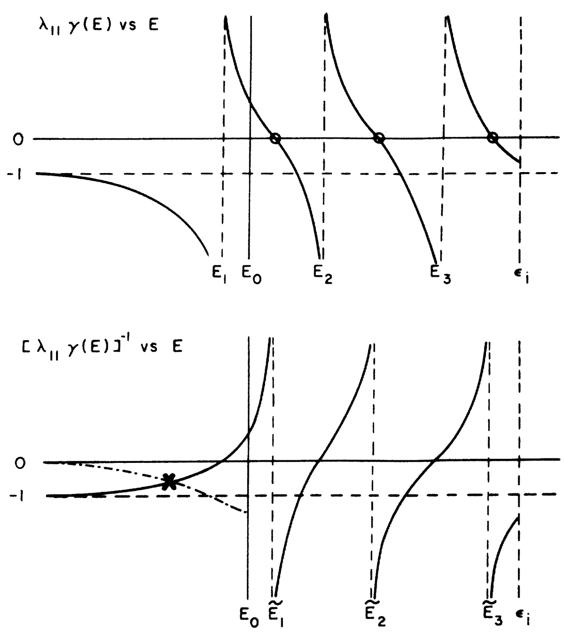

FIG. 11. The same as Fig. 9 except here the case where $\lambda=-1$ and $\lambda_{11}\gamma(\epsilon_i)<0$ is depicted.

$E=E_i<E_0$, and poles at the real energies $E=\tilde{E}_j$. In the Appendix we show that $D^{(+)}(E)$ can be constructed according to the prescription

$$D^{(+)}(E)=\prod_{i=1}^{N}\left(\frac{E-E_i}{E}\right)\prod_{j=1}^{M}\left(\frac{E}{E-\tilde{E}_j}\right)\times\exp\left[\frac{1}{\pi}\int_{E_0}^{\infty}\frac{\hat{\delta}(x)dx}{E-x+i_\epsilon}\right], \qquad (4.8)$$

where $D^{(+)}(E)$ has a series of zeroes at the N energies $E=E_i$, and a series of poles at the M energies $E=\tilde{E}_j$. The separable form factor will then have the form

$$\lambda_{11}[v(k_E)]^2=T(E)\prod_{i=1}^{N}\left(\frac{E-E_i}{E}\right)\prod_{j=1}^{M}\left(\frac{E}{E-\tilde{E}_j}\right)\times\exp\left[\frac{1}{\pi}\int_{E_0}^{\infty}\frac{\hat{\delta}(x)dx}{E-x+i\epsilon}\right]. \qquad (4.9)$$

In Fig. 13 we display the phase shift for a two-channel model problem with separable potentials in the form of Eq. (3.1). The potential $v_1(p)$ is again given by Eq. (3.6), with

$$\lambda_{11}=\lambda_{22}=-1,\quad \lambda_{12}=0.6,$$
$$c_2=c_3=750\ \text{MeV}/c,\quad \alpha_2=\alpha_3=400\ \text{MeV}/c\,.$$

These parameters produce a zero of $D^{(+)}(E)$ at

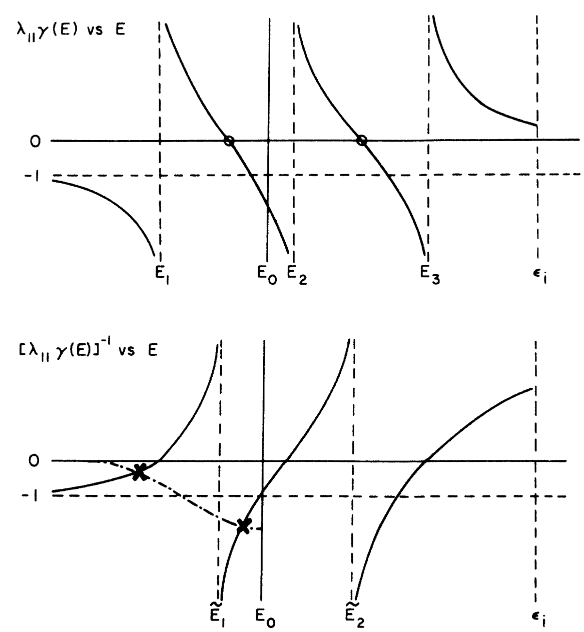

FIG. 12. The same as Fig. 9 except here the case where $\lambda_{11}=-1$ and $\lambda_{11}\gamma(\epsilon_i)>0$ is depicted. Notice that in this case, one has one less zero in $\gamma(E)$ [and hence $T(E)$] than poles. Also, in this case, $T(E)$ has two bound states poles (marked by "×") while $\lambda_{11}\gamma(E)$ has only one pole below elastic threshold E_0.

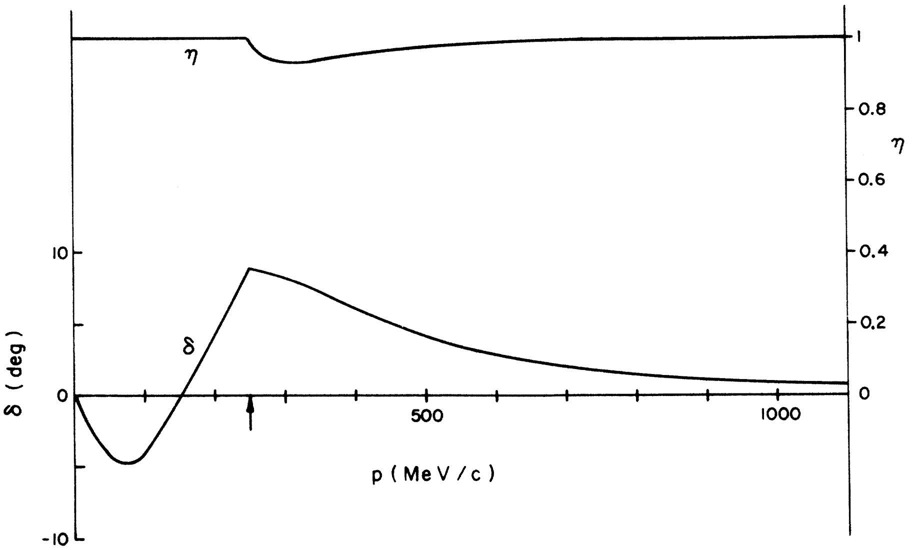

FIG. 13. The same as Fig. (5) except the parameters used are $\lambda_{11}=\lambda_{22}=-1$, $\lambda_{12}=0.6$, $c_2=c_3=750$ MeV/c, $\alpha_2=\alpha_3=$ 400 MeV/c. Notice that the phase shift changes sign below the inelastic threshold. The inverse procedure presented here has been tested numerically to recover $v_1(p)$ depicted in Fig. (3) from the phases presented in Figs. 4–6, 13.

$k=310i$ MeV/c, and a zero of the T matrix at $k=150$ MeV/c. Consequently, $v_1(k)$ was given by the equation

$$\lambda_{11}[v_1(k)]^2=T(E_k)\left[\frac{k^2+(310)^2}{k^2-(150)^2}\right]\times\exp\left[\frac{1}{\pi}\int_{E_0}^{\infty}\frac{\hat{\delta}(x)dx}{E_k+i\epsilon-x}\right]. \quad (4.10)$$

We repeat that the position of both the poles and zeroes of $T(E)$ must be specified in order to construct a unique separable potential which exactly reproduces the elastic phase shift. This is analogous to fixing the Castillejo, Dalitz, and Dyson ambiguity[17] in the solution of partial wave dispersion relations.

V. SUMMARY

In summary, we have seen that the existence of a many-channel potential of the form of Eq. (2.7) leads to an effective elastic channel potential $\lambda(E)\,v(k)\,v(k')$. For any elastic channel T matrix which is compatible with this underlying many-channel potential, one is able to construct $\lambda(E)\,v(k)\,v(k')$ analytically from Eq. (4.9). The T matrices may be quite varied, as can be seen from the examples presented. There are, however, limitations on the T matrices which can arise from a potential such as that given in Eq. (2.7). For T matrices which are inconsistent with this form of the coupled channel problem, one obviously cannot use the procedure presented here to generate an effective potential. There are certain cases where the T matrix has zeroes (i.e., the phase shifts change sign or pass through $n\pi$) that can be treated by this approach. In these cases, the zero of the T matrix is a consequence of a zero in the energy-dependent effective coupling constant $\gamma(E)$. For the case where $T(E)$ has no zeroes and $\hat{\delta}(E_0)=\hat{\delta}(\infty)$, the construction of $v(k)$ is identical to that of Ref. 9, although the conditions under which this construction has been shown to hold are not so restricted as in Ref. 9.

APPENDIX

In this appendix we derive the procedure [given in Eq. (4.8)] for constructing $D^{(+)}(E)$ in the case where $D^{(+)}(E)$ has zeroes and poles. We write the elastic scattering operator in terms of the function $D^{(+)}(E)$,

$$T=\frac{\lambda_{11}|v\rangle\langle v|}{D^{(+)}(E)}, \quad (A1)$$

where

$$D^{(+)}(E)=\frac{1}{\gamma(E)}-\lambda_{11}\langle v|G^{(+)}(E)|v\rangle \quad (A2)$$

and

$$\langle v|G^{(+)}(E)|v\rangle=\frac{1}{2\pi^2}\int_0^{\infty}\frac{k'^2dk'[v(k')]^2}{E+i\epsilon-Ek'}.$$

The fully on-shell T matrix $T(E)$ is defined by

$$T(E)=\frac{\lambda_{11}[v(k_E)]^2}{D^{(+)}(E)}. \quad (A3)$$

For complex energy z, the poles of $T(z)$ arise from zeroes of $D(z)$ [where $D^{(+)}(E) \equiv D(E+i\epsilon)$], and the zeroes of $T(z)$ arise from zeroes of $\gamma(z)$ and hence from *poles*[20] of $D(z)$. The distribution of poles and zeroes of $D(z)$ has been discussed extensively in the text. Briefly, the zeroes of $D(z)$ (which are marked by "×" in Figs. 9–12), occur for real energies below elastic threshold. The poles of $D(z)$ [which are zeroes of $\gamma(z)$ and are marked by "○" in Figs. 9–12], occur for real energies below the inelastic threshold. It will prove to be convenient to work in the momentum variable k_E rather than the energy variable E. We may consider D as a function of complex momentum $\bar{z}$. The zeroes and poles[16] of $D(\bar{z})$ clearly consist of bound state zeroes for $\bar{z}$ pure imaginary and poles which can occur for either $\bar{z}$ pure real or $\bar{z}$ pure imaginary. Since $D(\bar{z})$ is a function of $\bar{z}^2$, the zeroes and poles will occur in pairs which are symmetric about the origin.

Consider the case where $D(\bar{z})$ has a zero at $\bar{z}=\pm ik_B$ and a pole at $\bar{z}=\pm k_0$. Then we can construct a new function $\mathfrak{D}(\bar{z})$ which is analytic in the upper half $\bar{z}$ plane, viz.

$$\mathfrak{D}(\bar{z})=\frac{\bar{z}+\alpha}{\bar{z}-ik_B}\,\frac{\bar{z}^2-k_0^2}{(\bar{z}+\beta)(\bar{z}+\gamma)}D(\bar{z})\,. \tag{A4}$$

In Eq. (A4), α, β, and γ are arbitrary complex numbers with positive imaginary parts, hence $\mathfrak{D}(\bar{z})$ has *no pole* and *no zero* in the upper half of the $\bar{z}$ plane. Further, if $D(\bar{z})\to 1$ as $|\bar{z}|\to\infty$, then $\mathfrak{D}(\bar{z})\to 1$ as $|\bar{z}|\to\infty$, also.

Also, we have[21]

$$(k_E^2-k_0^2)D^{(+)}(E)=|(k_E^2-k_0^2)D^{(+)}(E)|\,e^{-i\hat{\delta}(k_E)}, \tag{A5}$$

where $\hat{\delta}(k_E)$ has been defined in Eq. (2.25).

From the properties of $\mathfrak{D}(\bar{z})$ we can see that $\ln[\mathfrak{D}(z)]$ will have no singularities in the upper half $\bar{z}$ plane, hence by Cauchy's theorem

$$\ln[\mathfrak{D}(\bar{z})]=\frac{1}{2\pi i}\int_c \frac{\ln[\mathfrak{D}(\bar{z}')]d\bar{z}'}{\bar{z}'-\bar{z}}\,, \tag{A6}$$

where $\bar{z}$ is in the upper half plane. This leads to

$$\mathrm{Re}\{\ln[\mathfrak{D}(k)]\}=\frac{P}{\pi}\int_{-\infty}^{\infty}\frac{dk'\,\mathrm{Im}\{\ln[\mathfrak{D}(k')]\}}{k'-k}\,. \tag{A7}$$

From Eqs. (A4) and (A5) we have

$$\mathrm{Im}\{\ln[\mathfrak{D}(k)]\}=\frac{1}{2i}\left[\ln\left(\frac{k+ik_B}{k-ik_B}\right)+\ln\left(\frac{k+\alpha}{k+\alpha^*}\right)+\ln\left(\frac{k+\beta^*}{k+\beta}\right)+\ln\left(\frac{k+\gamma^*}{k+\gamma}\right)\right]-\hat{\delta}(k)\,. \tag{A8}$$

Substituting this into Eq. (A7) we obtain

$$\mathrm{Re}\{\ln[\mathfrak{D}(k)]\}=\frac{\mathcal{P}}{2\pi i}\int_{-\infty}^{\infty}\frac{dk'}{k'-k}\left[\ln\left(\frac{k'+ik_B}{k'-ik_B}\right)+\ln\left(\frac{k'+\alpha}{k'+\alpha^*}\right)+\ln\left(\frac{k'+\beta^*}{k'+\beta}\right)+\ln\left(\frac{k'+\gamma^*}{k'+\gamma}\right)\right]-\frac{\mathcal{P}}{\pi}\int_{-\infty}^{\infty}\frac{\hat{\delta}(k')dk'}{k'-k}\,. \tag{A9}$$

The integrals in Eq. (A9) are of the form

$$I\equiv\frac{\mathcal{P}}{2\pi i}\int_{-\infty}^{\infty}\frac{dk'\ln[(k'+\alpha)/(k'+\alpha^*)]}{k'-k}\,, \tag{A10}$$

which we can rewrite as

$$I=\frac{\mathcal{P}}{2\pi i}\lim_{s\to 0^+}\int_{-\infty}^{\infty}\frac{dk'}{k'-k}\left[\ln\left(\frac{k'+\alpha}{k'+is}\right)+\ln\left(\frac{k'-is}{k'+\alpha^*}\right)\right]. \tag{A11}$$

The first term inside the square brackets in Eq. (A11) has no singularities in the upper half of the plane, and the second term has no singularities in the lower half plane. We can thus replace the principal value integral by adding or subtracting an imaginary term, viz.

$$I=\frac{1}{2\pi i}\lim_{s\to 0}\left\{\int_{-\infty}^{\infty}\frac{dk'\ln[(k'+\alpha)/(k'+is)]}{k'-k+i\epsilon}+i\pi\ln\left(\frac{k+\alpha}{k+is}\right)+\int_{-\infty}^{\infty}\frac{dk'n[(k'-is)/(k'+\alpha^*)]}{k'-k-i\epsilon}-i\pi\ln\left(\frac{k-is}{k+\alpha^*}\right)\right\}. \tag{A12}$$

The first integral in Eq. (A12) has no singularities in the upper half plane, so closing the contour in the upper half plane gives zero. Similarly, closing the second contour in the lower half plane gives zero. Taking the limit $s\to 0$ we find

$$I=\ln\left[\frac{|k+\alpha|}{k}\right], \tag{A13}$$

so that Eq. (A7) becomes

$$\mathrm{Re}\{\ln[\mathfrak{D}(k)]\} = \ln\left(\frac{|k+ik_B|\,|k+\alpha|}{k^2}\,\frac{k^2}{|k+\beta|\,|k+\gamma|}\right) - \frac{\mathcal{P}}{\pi}\int_{-\infty}^{\infty}\frac{\hat{\delta}(k')dk'}{k'-k}\,. \tag{A14}$$

Combining this with Eq. (A9), we find that

$$\ln[\mathfrak{D}(k)] = \ln\left[\frac{(k+ik_B)(k+\alpha)}{k^2}\,\frac{k^2}{(k+\beta)(k+\gamma)}\right] + \frac{1}{\pi}\int_{-\infty}^{\infty}\frac{\hat{\delta}(k')dk'}{k+i\epsilon-k'}\,. \tag{A15}$$

Substituting this into Eq. (A4) and solving for $D(k)$, we obtain

$$D(k) = \left(\frac{k^2+k_B^{\,2}}{k^2}\right)\left(\frac{k^2}{k^2-k_0^{\,2}}\right)\exp\left[\frac{1}{\pi}\int_{-\infty}^{\infty}\frac{\hat{\delta}(x)dx}{k+i\epsilon-x}\right]. \tag{A16}$$

Equation (A16) was derived for the case of one zero of $D(k)$ at $k=ik_B$ and a pair of poles at $k=\pm k_0$; it can obviously be extended to the case of N zeroes at $k=ik_i$ $(i=1, \ldots, N)$ and M poles at $k=\pm k_j$ $(j=1, \ldots, M)$ through the formula

$$D(k) = \prod_{i=1}^{N}\left(\frac{k^2+k_i^{\,2}}{k^2}\right)\prod_{j=1}^{M}\left(\frac{k^2}{k^2-k_j^{\,2}}\right) \times \exp\left[\frac{1}{\pi}\int_{-\infty}^{\infty}\frac{\hat{\delta}(x)dx}{k+i\epsilon-x}\right]. \tag{A17}$$

---

*Work supported in part by the National Science Foundation and the U.S. Atomic Energy Commission.

[1] NN separable potentials have been produced, among others, by F. Tabakin, Ann. Phys. (N. Y.) 30, 51 (1964); T. F. Hammann and Q. Ho-Kim, Nuovo Cimento 64B, 356 (1969); A. P. S. Sirohi and M. K. Srivastava, Nucl. Phys. A201, 66 (1973).

[2] A separable potential for $\bar{K}N$ scattering has been produced by M. Alberg, E. M. Henley, and L. Wilets, Phys. Rev. Lett. 30, 255 (1973).

[3] Separable potential for the ΛN-ΣN system has been proposed by E. Satah and Y. Nogami, Phys. Lett. 32B, 243 (1970).

[4] Separable potentials for NN, N-α, and α-α were constructed by J. Pigeon *et al.*, Phys. Rev. C 4, 704 (1971).

[5] R. Landau and F. Tabakin, Phys. Rev. D 5, 2746 (1972).

[6] M. G. Piepho and G. E. Walker, Phys. Rev. C 9, 1352 (1974).

[7] R. Omnes, Nuovo Cimento 8, 316 (1958).

[8] M. Gourdin and A. Martin, Nuovo Cimento 8, 699 (1958); M. Bolsterli and J. MacKenzie, Physics (N. Y.) 2, 141 (1965); H. Fiedeldey, Nucl. Phys. A135, 353 (1969).

[9] J. T. Londergan and E. J. Moniz, Phys. Lett. 45B, 195 (1973).

[10] J. T. Londergan, K. W. McVoy, and E. J. Moniz, to be published.

[11] H. Feshbach, Ann. Phys. (N.Y.) 5, 357 (1958).

[12] In Eq. (2.16), we have for convenience assumed nonrelativistic kinematics, i.e., $E=k^2/2\mu+\mu$, so that $\mu=k\,dk/dE$. If we used relativistic two-particle kinematics, i.e., $E=[k^2+m_1^{\,2}]^{1/2}+[k^2+m_2^{\,2}]^{1/2}$, this would amount to replacing μ by $k\,dk/dE$ in Eqs. (2.16)–(2.22).

[13] We cannot legitimately invert to obtain the potential for λ_{11} identically zero, as $D^{(+)}(E)$ does not approach 1 asymptotically. The actual problem considered is that for λ_{11} finite, but $\lim(\lambda_{11}/\lambda_{12})\to 0$.

[14] U. Amaldi, Rev. Mod. Phys. 39, 649 (1967).

[15] F. Tabakin, Ann. Phys. (N.Y.) 30, 51 (1964).

[16] It is possible to obtain singularities of $T(E)$ for energies above inelastic threshold by decoupling some inelastic channels. This possibility has been noted by L. Fonda and R. G. Newton, Ann. Phys. (N.Y.) 10, 490 (1960). We do not consider such "accidental" zeroes in this paper.

[17] L. Castillejo, R. H. Dalitz, and F. J. Dyson, Phys. Rev. 101, 453 (1956).

[18] N. Levinson, K. Dan. Vidensk. Selsk. Mat.–Fys. Medd. 25, No. 9 (1949).

[19] F. Tabakin, Phys. Rev. 177, 1443 (1969); M. Bolsterli, Phys. Rev. 182, 1095 (1969).

[20] In reducing the many-channel Hamiltonian to an equivalent one-channel problem, we formally eliminate the coupled channels, and, in so doing, we may introduce poles into the function $D(k)$. It is important to note that the Jost function for the many-channel problem has no such poles, and that the poles arise from eliminating the coupled inelastic channels. These poles arise from the zeroes of $\gamma(E)$ as has been demonstrated in Figs. 9–12.

[21] The definition of the phase $\hat{\delta}(E)$ has been chosen such that is is continuous when the elastic scattering T matrix passes through zero. If one chooses as the phase shift the phase of $D^{(+)}(k)$, then, as noted in M. Bolsterli, Phys. Rev. 182, 1095 (1969), the phase would be discontinuous at the zeroes of T.